H3K9 acetylation-dependent *CHAC1* transcription in dihydroartemisinin-induced hepatic stellate cell ferroptosis

Min Shen[1,2,3], Wenshu Han[1], Liangliang Cai[1,2,3], Weijuan Gong[1,2,3], Li Qian[1,2,3]

[1]Institute of Translational Medicine, School of Medicine, Yangzhou University, Yangzhou, Jiangsu 225009, China;
[2]Department of Gastroenterology, The Affiliated Hospital of Yangzhou University, Yangzhou University, Yangzhou, Jiangsu 225009, China;
[3]The Key Laboratory of the Jiangsu Higher Education Institutions for Integrated Traditional Chinese and Western Medicine in Senile Diseases Control, Yangzhou University, Yangzhou, Jiangsu 225009, China.

Abstract

Background: The activation of hepatic stellate cells (HSCs) plays a crucial role in the progression of liver fibrosis, and eliminating activated HSCs is regarded as an effective strategy for combating fibrosis. Ferroptosis has emerged as a potential mechanism for HSC depletion. Dihydroartemisinin (DHA), a derivative of artemisinin, has shown anti-fibrotic effects, but its role in HSC ferroptosis remains unclear. This study aimed to investigate the molecular mechanism by which DHA regulates HSC ferroptosis through histone modifications to suppress liver fibrosis.

Methods: *In vitro* experiments were conducted using human hepatic stellate cell line HSC-LX2 and mouse hepatic stellate cell line mHSC, with DHA treatment to induce ferroptosis, and ferrostatin-1 as a ferroptosis inhibitor for control. RNA sequencing was performed to analyse differentially expressed genes in DHA-treated HSCs, and real-time polymerase chain reaction, Western blotting, and immunofluorescence were used to verify glutathione-specific gamma-glutamylcyclotransferase 1 (CHAC1) expression. Chromatin immunoprecipitation quantitative polymerase chain reaction was used to detect histone acetylation at the *CHAC1* promoter, and luciferase reporter assays with wild-type or mutated *CHAC1* promoter were used to confirm activating transcription factor 4 (ATF4) binding sites. *In vivo* experiments used male C57BL/6J mice induced with carbon tetrachloride (CCl_4) to establish a liver fibrosis model. Histopathological staining, serum biochemical index detection, and ferroptosis-related assays in isolated liver cells were performed to evaluate the therapeutic effect of DHA and the roles of CHAC1 and ATF4.

Results: DHA inhibited HSC activation through the ferroptosis pathway, DHA treatment elevated *CHAC1* levels in HSCs, inhibition of CHAC1 prevented DHA-induced HSC ferroptosis, and DHA regulated the expression of *CHAC1* at the transcriptional level rather than at the post-transcriptional level in HSC-LX2 and mHSC cells. Mechanistically, upregulated H3K9 acetylation was essential for the DHA-mediated transcriptional upregulation of *CHAC1* through increased histone acetyltransferase P300 in HSCs. Inhibiting histone acetylation attenuated DHA-induced CHAC1 upregulation and ferroptosis. ATF4 was identified as a key transcription factor in the transcriptional activation of *CHAC1*. Interfering with ATF4 inhibited the transcriptional upregulation of *CHAC1* by DHA. Notably, the −212 to −199 bp and −269 to −257 bp promoter regions in *CHAC1* were essential for the initiation of transcription of ATF4. In mice, treatment with DHA alleviated murine liver fibrosis by inducing HSC ferroptosis. Inhibition of CHAC1 or ATF4 impaired DHA-induced HSC ferroptosis in murine liver fibrosis.

Conclusion: The transcriptional activation of *CHAC1*, which is regulated by H3K9 acetylation, was essential for the ability of DHA to trigger HSC ferroptosis and, consequently, to suppress liver fibrosis.

Keywords: Dihydroartemisinin; Ferroptosis; Hepatic stellate cell; Glutathione-specific gamma-glutamylcyclotransferase 1; Histone acetylation; Liver fibrosis; Aactivating transcription factor 4

Introduction

Liver fibrosis represents a prevalent pathological condition that is often observed in the progression of various chronic liver diseases.[1] The progression of liver fibrosis is complex and involves multiple elements, with the activation of hepatic stellate cells (HSCs) serving as a vital factor that has been extensively investigated in previous studies.[2] Therefore, the prevention of activated HSCs has emerged as a highly promising approach for addressing the challenges associated with liver fibrosis.[3] Clinical research has revealed that individuals with chronic hepatitis typically exhibit mild to moderate iron accumulation, which can stimulate the production of type IV collagen, leading to the development of fibrosis enveloped by iron within the liver.[4] Importantly, research has shown that hepatic fibrosis can be effectively addressed through the targeted induction of death in activated HSCs by

Access this article online

Quick Response Code:

Website: www.cmj.org

DOI: 10.1097/CM9.0000000000003788

Correspondence to: Li Qian, Institute of Translational Medicine, School of Medicine, Yangzhou University, 88 University South Road, Yangzhou, Jiangsu 225009, China
E-Mail: qianl@yzu.edu.cn

Chinese Medical Journal 2026;139(1)
Received: 24-07-2025; **Online:** 15-09-2025 **Edited by:** Xuehong Zhang

modulating the process of ferroptosis.[5] Dihydroartemisinin (DHA) is a natural antimalarial medication that is generally well tolerated and has a wide range of pharmacological benefits, including antibacterial, antitumor, and antischistosomiasis activities. Studies indicate that DHA exerts antihepatic fibrosis effects by inducing HSC ferroptosis.[6] This research explored in greater detail the mechanisms by which DHA triggers ferroptosis in HSCs and assessed its impact on the suppression of liver fibrosis.

Ferroptosis, a newly discovered form of regulated cell death, has been investigated in cancer and cancer treatment.[7] During ferroptosis, decreased cellular glutathione (GSH) levels lead to the accumulation of lipid reactive oxygen species (ROS) and ultimately cause cell death.[8,9] Several intracellular signaling molecules and signaling pathways, such as glutathione peroxidase 4 (GPX4),[10] cystine-glutamate antiporter (system Xc^-),[11] and p62–Kelch-like ECH-associated protein 1–nuclear factor E2 related factor 2 pathways,[12] have been suggested to mediate this process through regulating GSH levels. The glutathione-specific gamma-glutamylcyclotransferase 1 (*CHAC1*) gene is recognized as a promising candidate gene involved in the GSH metabolism signaling pathway. This enzyme facilitates the hydrolysis of GSH within the cytosol of mammalian cells through its γ-glutamylcyclotransferase activity, converting GSH into 5-oxoproline and cysteinyl glycine. This process plays a significant role in the regulation of GSH levels and the overall metabolism of thiol compounds in cellular environments.[13] *CHAC1* has a structure butirosin resistance regulatory protein G/γ-glutamyl cyclotransferase (BtrG/γ-GCT fold) and an active site similar to that of γ-GCT and mediates the degradation of cellular GSH. When *CHAC1* is overexpressed, it results in a reduction in intracellular GSH, an increase in ROS levels, and a decrease in GPX4 protein levels.[14] In this study, we found that DHA significantly upregulated the transcriptional level of *CHAC1* but did not affect its posttranscriptional level. However, the role of transcriptional regulation in DHA-induced ferroptosis remains incompletely understood.

Acetylation of lysine residues on histones plays a crucial role in modifying chromatin in relation to gene expression. This process can diminish the positive charge associated with the ε-amino groups of lysine, thereby reducing the interactions between histones and DNA within the nucleosome structure.[15] Histone acetylation is a process facilitated by enzymes known as histone acetyltransferases (HATs). This modification is critical because it plays a significant role in the regulation of gene expression and the overall structure of chromatin. Conversely, histone deacetylation by histone deacetylases (HDACs) results in transcriptional repression. Histone acetylation occurs at multiple sites, including K9, K14, K18, K23, and K27 in histone H3, as well as K5, K8, K12, and K16 in histone H4.[16] Notably, previous studies reported that histone modifications at histone H3 lysine 27 (H3K27),[17] histone H3 lysine 9 (H3K9),[18] and histone H4 lysine 8 (H4K8)[19] are involved in the activation of HSCs and liver injury, but the specific mechanism is unclear. Consequently, we investigated the correlation between these three modification sites and DHA-induced ferroptosis in HSCs.

In this study, we aimed to investigate the molecular mechanism by which DHA regulates *CHAC1* transcription through H3K9 acetylation (H3K9ac) to induce ferroptosis in HSCs.

Methods

Animal experiments

The experimental protocols involving animals were thoroughly examined and received the necessary approval from the Institutional Animal Care and Use Committee at Yangzhou University (No. 202410030). The study used male C57BL/6J mice, each weighing 18–22 g, which were bred and kept in a controlled environment devoid of specific pathogens. In line with established research methodologies,[20] from weeks 1 to 8, a mixture of carbon tetrachloride (CCl_4) and olive oil at a 1:9 volumetric ratio was administered via intraperitoneal injection (0.1 mL/20 g body weight, 3 times/week). This procedure was implemented to effectively induce hepatic fibrosis in the subjects. A total of five groups of mice were subjected to various treatments to evaluate the effects of different interventions. These groups included vehicle + control-vector, CCl_4 + control-vector, CCl_4 + control-vector + DHA, CCl_4 + adeno-associated virus serotype 8 (AAV8)-*Chac1*-short hairpin RNA (shRNA) + DHA, and CCl_4 + AAV8-activating transcription factor 4 (*Atf4*)-shRNA + DHA. DHA, which was used at a dosage of 20 mg/kg, was administered by dissolving it in olive oil and delivering it via intraperitoneal injection once daily over a duration of 5 to 8 weeks. Vectors of AAV8 were generated and administered to mice through the caudal vein.[21] At the end of the experiment, blood and liver samples were collected from each group. The liver tissues were preserved in a 4% paraformaldehyde solution for histopathological examination.

Histological analyses

The harvested liver tissue was fixed in a 4% paraformaldehyde solution (PFA), followed by gradient dehydration and embedding in paraffin. In line with our previous findings, liver sections of 4 μm thickness were stained with hematoxylin and eosin (H&E), and Masson and Sirius Red staining were also conducted. Immunohistochemical staining for alpha-smooth muscle actin (α-SMA) was performed as previously described.[6]

RNA sequencing

Total RNA was extracted from HSC-LX2 cells (BeNa Culture Collection, Beijing, China) through TRIzol reagent (Invitrogen, Carlsbad, CA, USA). For library preparation, 1 μg of RNA from each sample was extracted with the TruSeq Stranded Total RNA and Ribo-Zero Gold Kit (MRZG12324, Illumina, San Diego, California, USA). The reads for each sample were aligned to the human reference genome (GRCh38.p10) via TopHat v1.4.1 (Johns Hopkins University, MD, USA). Differential gene expression analysis was conducted via DESeq2 (https://github.com/mikelove/DESeq2). To compute the adjusted *P* values, the Benjamini–Hochberg method was applied.

We used a fold change <–2 for downregulation and a fold change >2 for upregulation as cut-offs.

Chemicals and antibodies

Primary antibodies against α-SMA (A1011), collagen I (A1352), fibronectin (A16678), H4K8 acetylation (H4K8ac, A7258), H3K9ac (A7255), H3K27 acetylation (H3K27ac, A7253), and β-actin (AC038) were obtained from ABclonal (Wuhan, China). Cycloheximide (CHX, C7698) and actinomycin D (Act-D, A9415) were obtained from Sigma–Aldrich (MO, USA). Primary antibodies against GPX4 (ET1706-45) were obtained from HuaBio (Hangzhou, China).

Plasmid construction

pcDNA3.1-*CHAC1* was obtained from Genechem (Shanghai, China). In accordance with our previous reports, PLKO.1-sh*CHAC1* and PLKO.1-sh*ATF4* were synthesized by Tsingke Biotech (Beijing, China).[6]

Cell culture

Primary HSCs were isolated from male C57BL/6J mice following established protocols as detailed in previous studies.[22] In addition, the activated HSC line HSC-LX2, as well as activated mouse HSCs (mHSCs), were obtained from BeNa Culture Collection (Beijing, China). Both HSC-LX2 cells and mHSCs were cultured in Dulbecco's modified Eagle medium supplemented with 1% antibiotics and 10% fetal bovine serum. The cultures were incubated at 37°C in a humidified atmosphere of 5% carbon dioxide.

Western blotting

To homogenize the collected cells, radio immunoprecipitation assay (RIPA) buffer supplemented with protease inhibitors was used. Following this step, the concentration of the proteins was quantified through the bicinchoninic acid (BCA) colorimetric assay. Subsequently, 5 × sodium dodecyl sulfate (SDS) loading buffer (P0015L, Beyotime Biotechnology, Shanghai, China) was added to the samples, which were boiled for 10 minutes. After the samples were subjected to SDS–polyacrylamide gel electrophoresis (PAGE) for protein separation, the proteins were transferred onto polyvinylidene fluoride (PVDF) membranes. The immunoblots were incubated for 1 hour at room temperature in a blocking solution of 5% bovine serum albumin (BSA), followed by three washes with tris-buffered saline with tween (TBST). The samples were subsequently incubated overnight with the primary antibody at 4°C. After three additional washes in TBST with 0.1% Tween 20, the blots were treated with the secondary antibody at room temperature for 1 hour.

RNA extraction and real-time polymerase chain reaction (PCR)

Following the provided guidelines, RNA was extracted from HSC-LX2 cells with TRIzol reagent (15596018, Invitrogen, Carlsbad, CA, USA). A complementary DNA (cDNA) synthesis kit (11123ES60, Yeasen Biotechnology, Shanghai, China) was subsequently used for reverse transcription to generate cDNA. For real-time PCR, the synergetic binding reagent Green PCR kit (11202ES08, Yeasen Biotechnology) was used in accordance with the manufacturer's instructions. The following primers were used: human-*CHAC1* forward primer, 5′-GCTGTGGATTTTCGGGTACG-3′; and human-*CHAC1* reverse primer, 5′-CACACG GCCAGGCATCTT-3′; $2^{-\Delta\Delta Ct}$ was used to calculate the fold change in messenger RNA (mRNA) expression.

Immunofluorescence

In a 24-well cell culture plate, HSCs were initially plated and subsequently treated with appropriate reagents for 24 h. Following this treatment, the cells were collected and fixed with 4% PFA for 15 min, after which they were incubated in 1% BSA for 20 min. The cells were subsequently incubated with primary antibodies overnight at 4°C. Next, the sections were incubated with fluorescein isothiocyanate (FITC)-conjugated secondary antibodies at room temperature for 2 hours. Finally, 4′,6-diamidino-2-phenylindole (DAPI, KGA215-50, KeyGEN BioTECH, Nanjing, China) was used to stain the cell nuclei, which were then imaged via fluorescence microscopy.

Iron assay

In accordance with the manufacturer's instructions, an iron assay kit was used to assess the relative levels of iron present in the cell lysates (DojinDo, Kumamoto, Japan).[23]

Lipid peroxidation assay

Following the manufacturer's guidelines, we used a lipid peroxidation assay kit (S0131S, Beyotime Biotechnology) to assess the levels of lipid peroxidation by measuring the malondialdehyde (MDA) product within the cell lysates.

ROS assay

For the assay, BODIPY 581/591 C11 (D3861, Thermo Fisher, Waltham, USA) was used to identify lipid peroxidation. The HSCs were treated with the compounds for 24 h, followed by a 30-min staining period using BODIPY 581/591 C11.

GSH assay

Following the guidelines set by the manufacturer, the relative GSH concentration was measured with the use of a GSH assay kit (S0053, Beyotime Biotechnology).

Protein stability

The stability of the CHAC1 protein was assessed through the use of CHX. For the assay, HSC-LX2 cells were treated with CHX at a concentration of 100 μg/mL for a specified duration, after which the protein levels of CHAC1 were quantified by Western blotting analysis.

RNA stability

CHAC1 mRNA stability was assessed via Act-D (5 μg/mL) according to a previous study.[24] Following incubation for the specified durations, HSC-LX2 cells were collected and total RNA was extracted for real-time PCR analysis.

Chromatin immunoprecipitation quantitative polymerase chain reaction (ChIP-qPCR)

Immunoprecipitation reactions were conducted via the sonication ChIP kit from ABclonal Technology. For each immunoprecipitation reaction, a total of 2×10^6 cells were used to ensure a sufficient amount of material for analysis. Next, for ChIP-qPCR, both the input DNA and the immunoprecipitated DNA were quantified through real-time qPCR techniques. To ensure accurate comparison and analysis, each sample of ChIP DNA was normalized on the basis of the corresponding input DNA levels, allowing for reliable interpretation of the results.

Luciferase reporter system construction

As described previously,[25] the *CHAC1* promoter (–500 to +1, –212 to –199 bp mutation, –269 to –257 bp mutation) was cloned and inserted into the pGL3 luciferase reporter (pGL3-Luc) vector. Then, the pGL3-Luc, pGL3-Luc-*CHAC1*-wild type (WT), pGL3-Luc-*CHAC1*-mution (Mut)1, pGL3-Luc-*CHAC1*-Mut2, and pGL3-Luc-*CHAC1*-Mut3 plasmids were transfected into the cells. To assess the efficiency of transfection, cells were transfected with luciferase reporter vectors alongside phRL-null. The promoter region targeted by transcription factor binding was predicted through JASPAR (http://jaspar.genereg.net/) and the UCSC Genome Browser (https://genome.ucsc.edu/index.html).

Statistical analysis

In this study, all quantitative data are continuous variables and are presented as the mean ± standard error of the mean. All datasets were confirmed to follow a normal distribution. The statistical comparisons between two groups or among several groups were assessed through Student's *t*-test or one-way analysis of variance, with subsequent application of the Student–Newman–Keuls test. All the statistical analyses were conducted through GraphPad Prism 8 (California, San Diego, USA). A P value <0.05 indicated statistical significance in all analyses.

Results

CHAC1 expression is upregulated during DHA-induced HSC ferroptosis

Previous research has demonstrated that DHA ameliorates liver histopathological damage and suppresses the progression of liver fibrosis by triggering ferroptosis in HSCs.[6] In agreement with earlier findings, we found that DHA inhibited the levels of the activation markers alpha-smooth muscle actin (*ACTA2*), collagen I (*COL1A1*), and fibronectin in HSC-LX2 cells [Figure 1A, Figure 1B, and Supplementary Figure 1A, http://links.lww.com/CM9/C590]. Lipid ROS accumulation, iron overload, lipid peroxidation, and GSH depletion are hallmarks of ferroptotic cells. As expected, treatment with DHA dramatically increased the level of the lipid peroxidation product MDA, lipid ROS and intracellular redox-active iron and decreased the level of GSH [Figure 1C–F]. Crucially, ferrostatin-1 (Fer-1) notably disrupts these typical ferroptotic processes, which involve an overload of intracellular redox-active iron, the generation of MDA, the accumulation of ROS, a decrease in GSH levels, and a decrease in the cell status of HSCs [Figure 1C–F and Supplementary Figure 1B, http://links.lww.com/CM9/C590]. Overall, these results confirm that DHA can trigger HSC ferroptosis *in vitro*.

The prevention and treatment of ferroptosis through traditional Chinese medicine is gaining increasing attention. Cystine depletion, inhibition of system Xc^- and inactivation of GPX4 can induce ferroptosis. This raises the question of how DHA regulates ferroptosis. To investigate this question, we conducted RNA sequencing. The results reveal that 398 mRNAs were significantly increased (fold change >2), whereas 889 mRNAs were decreased (fold change <–2) in the DHA-treated HSC-LX2 cells [Figure 1G and Supplementary Figure 1C, http://links.lww.com/CM9/C590]. Among these upregulated genes associated with ferroptosis, the change in *CHAC1* was the most obvious. The real-time PCR, Western blotting, and immunofluorescence assay results reveal that DHA treatment upregulated CHAC1 in a dose-dependent manner in both HSC-LX2 cells and mHSCs [Figure 1H–K and Supplementary Figure 1D and E, http://links.lww.com/CM9/C590]. Overall, these results reveal that CHAC1 expression is upregulated during DHA-induced HSC ferroptosis.

Downregulation of CHAC1 expression inhibits DHA-induced HSC ferroptosis

Several evidence suggest that increased CHAC1 expression is related to ferroptosis.[13,26] To determine whether upregulated CHAC1 expression contributes to DHA-induced HSC ferroptosis, a lentiviral packaging system was used to establish *CHAC1*-knockdown HSC-LX2 cell lines [Supplementary Figure 2A, http://links.lww.com/CM9/C590]. As expected, *CHAC1* knockdown dramatically abolished the DHA-induced inhibition of cell growth [Figure 2A]. The *CHAC1* knockdown had no significant effect on HSC ferroptosis, but decreased DHA-induced MDA production, redox-active iron accumulation, lipid ROS generation, and GSH depletion [Figure 2B–F and Supplementary Figure 2B, http://links.lww.com/CM9/C590]. Treatment with DHA induced mitochondrial shrinkage and increased the mitochondrial membrane density. However, transfection of HSC-LX2 cells with sh*CHAC1* abolished the typical changes observed in ferroptotic cells [Figure 2G]. CHAC1 has been found to decrease intracellular GSH levels, and GSH depletion subsequently inhibits the activity of the GPX4 enzyme, thereby inducing ferroptosis.[13] Furthermore, Western blotting analysis showed that DHA treatment inhibited GPX4 expression by upregulating CHAC1, whereas CHAC1 downregulation disrupted the regulatory effect of DHA on GPX4 [Figure 2H].

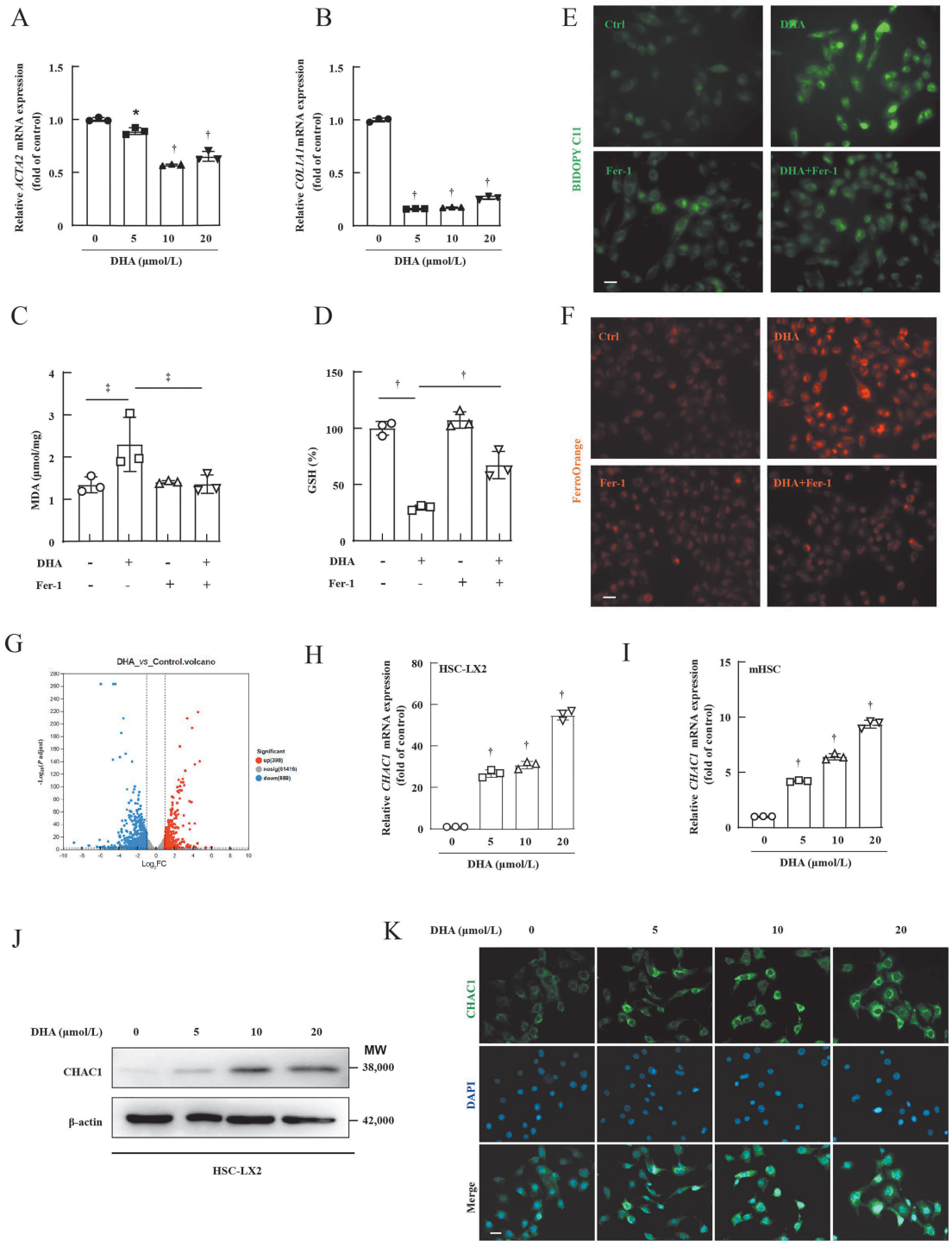

Figure 1: CHAC1 expression is upregulated during DHA-induced HSC ferroptosis. (A and B) The levels of *ACTA2* and *COL1A1* were measured through real-time PCR in HSC-LX2 cells. (C–F) HSC-LX2 cells were treated with DHA (20 μmol/L) for 24 h and Fer-1 (1 μmol/L) for 24 h. The levels of MDA, GSH, ROS, and intracellular iron were detected. (G) The volcano plot of HSC-LX2 cells were treated with DHA (20 μmol/L) for 24 h. (H and I) The mRNA levels of *CHAC1* in HSC-LX2 cells and mHSCs were treated with DHA (5, 10, or 20 μmol/L) for 24 h. (J) CHAC1 levels were measured by Western blotting. (K) Immunofluorescence was used to detect the expression of CHAC1 in mHSCs. scale bars: 20 μm, $n = 3$ in every group. $^{*}P < 0.01$; $^{\dagger}P < 0.001$; $^{\ddagger}P < 0.05$. *ACTA2*: Alpha-smooth muscle actin; CHAC1: Glutathione-specific gamma-glutamylcyclotransferase 1; *COL1A1*: Collagen Ⅰ; Ctrl: Control; DAPI: 4′,6-diamidino-2′-phenylindole; DHA: Dihydroartemisinin; Fer-1: Ferrostatin-1; HSC: Hepatic stellate cell; GSH: Glutathione; MDA: Malondialdehyde; mHSC: Mouse hepatic stellate cell; MW: Molecular weight; PCR: Polymerase chain reaction; ROS: Reactive oxygen species.

The activation markers of HSCs, specifically α-SMA, fibronectin, and collagen Ⅰ, were subsequently evaluated and identified. As shown in Figure 2I and Supplementary Figure 2C and D, http://links.lww.com/CM9/C590, a decrease in the expression of these markers related to HSC activation was detected. Conversely, *CHAC1* knockdown effectively reversed the suppressive effect of DHA on HSC activation. Collectively, these results support that downregulated CHAC1 expression could inhibit DHA-induced HSC ferroptosis.

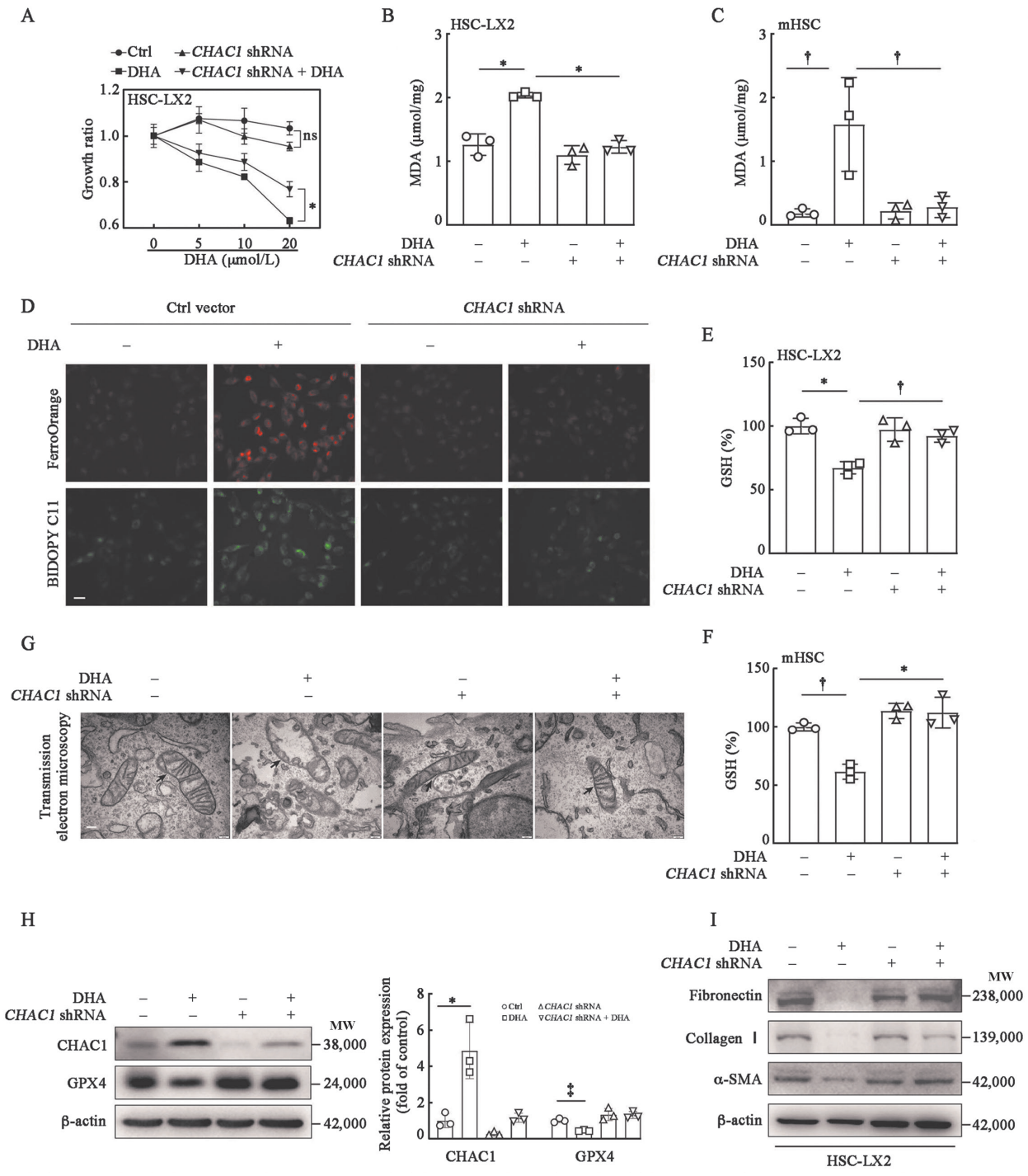

Figure 2: Downregulation of CHAC1 expression inhibited DHA-induced HSC ferroptosis. (A) Cell counting kit-8 was used to determine cell viability in HSC-LX2 cells. (B–F) MDA production, iron accumulation, lipid ROS levels, and GSH depletion were assayed in HSC-LX2 cells and mHSCs. Scale bars: 20 μm. (G) Transmission electron microscopy was used to examine the typical changes in ferroptotic cells. Arrows show characteristic mitochondrial alterations. Scale bars: 0.2 μm. (H) The levels of CHAC1 and GPX4 were measured by Western blotting. (I) Western blotting analysis of the protein levels of α-SMA, collagen Ⅰ, and fibronectin. $^{*}P<0.001$; $^{\dagger}P<0.01$; $^{\ddagger}P<0.05$. α-SMA: Alpha-smooth muscle actin; CHAC1: Glutathione-specific gamma-glutamylcyclotransferase 1; Ctrl: Control; DHA: Dihydroartemisinin; GPX4: Glutathione peroxidase 4; GSH: Glutathione; HSC: Hepatic stellate cell; MDA: Malondialdehyde; mHSC: Mouse hepatic stellate cell; MW: Molecular weight; ns: Not significant; ROS: Reactive oxygen species; shRNA: Short hairpin RNA.

Upregulated H3K9 acetylation is essential for the transcriptional activation of CHAC1 induced by DHA in HSCs

How does DHA regulated the expression of CHAC1? To explore this question, we initially examined whether DHA affects the protein level of CHAC1. However, the CHX chase assay revealed that there was no significant effect on the half-life of the CHAC1 protein during DHA-induced ferroptosis in HSC-LX2 cells [Figure 3A and B]. Similarly, the mRNA half-life of *CHAC1* in HSC-LX2 cells exposed to the translation inhibitor Act-D did not notably differ from that in control cells or those treated with DHA [Figure 3C]. These results suggested that DHA regulated the transcriptional level rather than the posttranscriptional level of CHAC1.

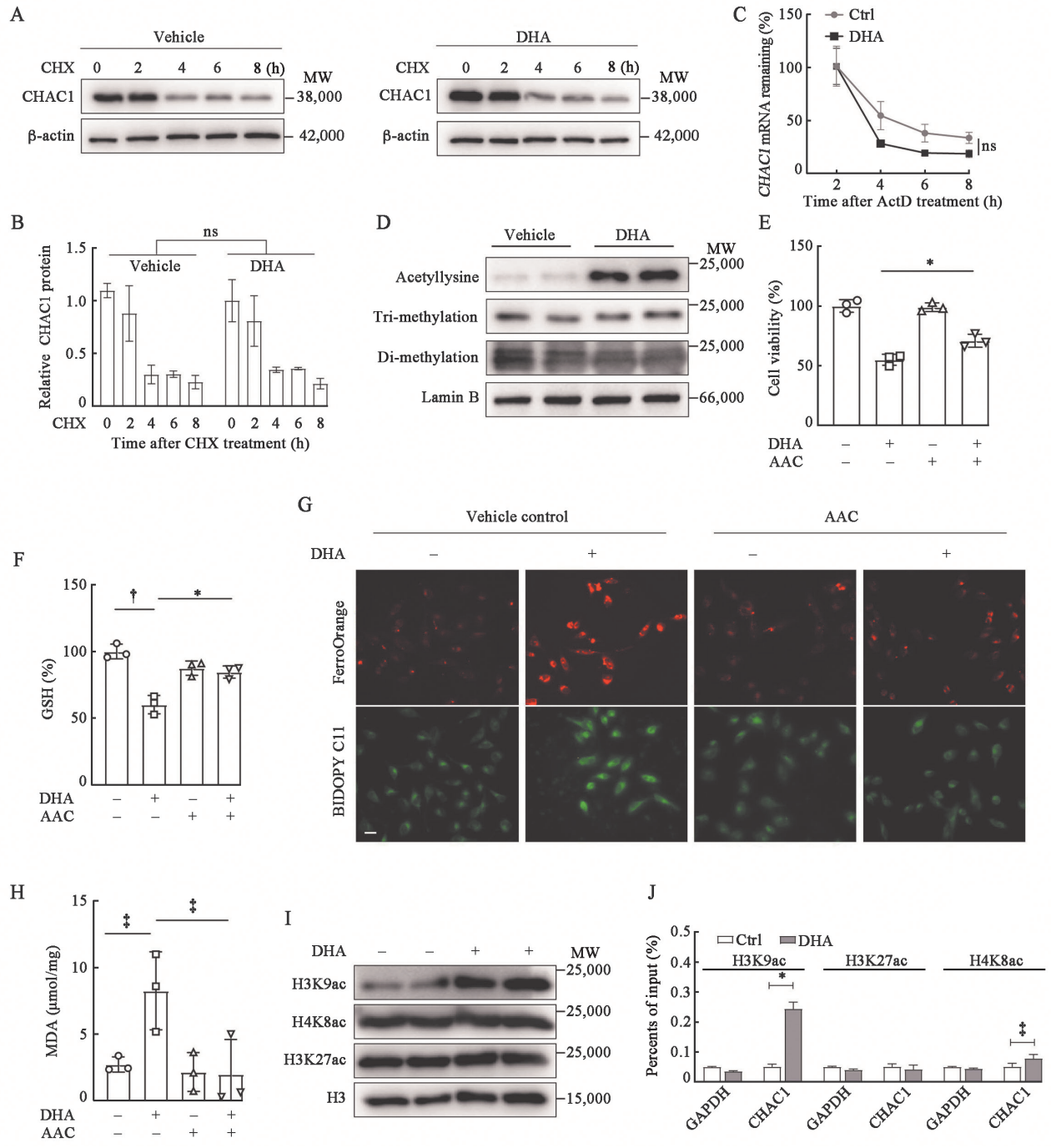

Figure 3: Upregulated H3K9 acetylation is essential for the transcriptional activation of *CHAC1* induced by DHA in HSCs. (A and B) The protein level of CHAC1 in HSC-LX2 cells with DHA (20 μmol/L) for 24 h and then treated with 100 μg/mL CHX for the indicated times were determined by Western blotting. (C) The level of remaining *CHAC1* messenger RNA was measured in HSC-LX2 cells with DHA (20 μmol/L) for 24 h and then treated with 5 μg/mL Act-D for the indicated times via real-time PCR. (D) The levels of acetyllysine, tri-methylated and di-methylated acetyllysine in HSC-LX2 cells with DHA (20 μmol/L) for 24 h were detected by Western blotting. (E) Cell counting kit-8 was used to determine the viability in HSC-LX2 cells. (F–H) GSH depletion, iron accumulation, lipid ROS levels, and MDA production were assayed in HSC-LX2 cells. Scale bars: 20 μm. (I) H3K9ac, H4K8ac, and H3K27ac levels were detected by Western blotting in HSC-LX2 cells. (J) ChIP-qPCR was used to measure the H3K9ac, H4K8ac, and H3K27ac modifications of CHAC1 in HSC-LX2 cells. $n = 3$ in every group. $^{*}P < 0.01$; $^{\dagger}P < 0.001$; $^{\ddagger}P < 0.05$. AAC: Anacardic acid; Act-D: Actinomycin D; CHAC1: Glutathione-specific gamma-glutamylcyclotransferase 1; ChIP-qPCR: Chromatin immunoprecipitation quantitative polymerase chain reaction; CHX: Cycloheximide; Ctrl: Control; DHA: Dihydroartemisinin; H4K8ac: Histone H4 lysine 8 acetylation; HSC: Hepatic stellate cell; H3K9ac: Histone H3 lysine 9 acetylation; H3K27ac: Histone H3 lysine 27 acetylation; GSH: Glutathione; MDA: Malondialdehyde; MW: Molecular weight; PCR: Polymerase chain reaction; ROS: Reactive oxygen species.

Histone modifications, including acetylation and methylation, play a central role in genome regulation and transgenerational epigenetic inheritance. To investigate whether histone modification is involved in the regulation of *CHAC1* in DHA-induced HSC ferroptosis, we first examined the levels of acetylation and methylation of histones during DHA-induced HSC ferroptosis. The results revealed a significant increase in histone acetylation levels after treatment with DHA [Figure 3D]. Notably, the level of the acetylase E1A binding protein p300 (EP300) was

significantly increased, but there were no large differences in the levels of other HDACs [Supplementary Figure 3A and B, http://links.lww.com/CM9/C590]. Anacardic acid (AAC) has been shown to inhibit the activity of the HAT EP300. AAC was subsequently applied as a treatment for reverse verification, followed by DHA treatment. The results indicated that the expression of EP300, histone acetylation, and CHAC1 could be rescued by AAC under DHA treatment [Supplementary Figure 2A and C–E, http://links.lww.com/CM9/C590]. Next, several ferroptotic events were detected, and the results showed that AAC treatment restored the cellular state and cell viability and inhibited ferroptotic events induced by DHA, including GSH reduction, redox-active iron accumulation, lipid ROS generation, and MDA production [Figure 3E–H and Supplementary Figure 3F, http://links.lww.com/CM9/C590]. Moreover, inhibiting histone acetylation by AAC abrogated the DHA-induced increases in CHAC1 and GPX4 expression [Supplementary Figure 3G, http://links.lww.com/CM9/C590]. H3K27, H3K9, and H4K8 are reportedly involved in the activation of HSCs. To investigate which lysine site is primarily regulated by DHA in terms of histone acetylation, we used Western blotting to detect histone acetylation sites in HSC-LX2. The results indicated that H3K9 acetylation was significantly increased following DHA treatment [Figure 3I]. In addition, ChIP–qPCR demonstrated that the acetylation level of *CHAC1* was significantly increased at H3K9, whereas no significant changes were detected at H3K27 or H4K8 [Figure 3J]. These results showed that DHA could further upregulate H3K9 acetylation, thereby promoting *CHAC1* transcription, which could contribute to HSC ferroptosis.

ATF4 is involved in regulating CHAC1 transcription through H3K9 acetylation

Histone acetylation plays a crucial role in transcriptional activation by modulating the binding activity of transcription factors.[27] To address which transcription factors are involved in H3K9 acetylation-regulated *CHAC1* transcription under DHA treatment, we used online databases (https://genome.ucsc.edu/) to analyze potential transcription factors associated with CHAC1 and conducted a co-analysis with the RNA sequencing results [Figure 4A]. Our findings suggested that CEBPB and ATF4 may act as transcription factors that regulate *CHAC1* transcription in response to DHA. Notably, interference with CEBPB did not significantly affect CHAC1 expression, whereas interference with ATF4 resulted in substantial inhibition of CHAC1 transcription [Figure 4B and C, Supplementary Figure 3H, http://links.lww.com/CM9/C590]. In addition, there was no significant change in H3K9 acetylation of the transcription factors ATF4, and CEBPB [Supplementary Figure 3I, http://links.lww.com/CM9/C590]. It indicated that under DHA treatment, H3K9 acetylation directly regulates CHAC1 expression by altering chromatin accessibility, rather than through the CHAC1 transcription factor ATF4 or CEBPB. We next investigated whether ATF4 is involved in DHA-induced HSC ferroptosis. The results indicated that ATF4 knockdown decreased DHA-induced GSH reduction, redox-active iron accumulation, lipid ROS generation, and MDA production in both HSC-LX2 cells and mHSC [Figure 4D–H]. Taken together, these findings indicated that ATF4 played a critical role in the regulation of *CHAC1* transcription mediated by H3K9 acetylation, which in turn influences HSC ferroptosis and activation.

ATF4 promotes the transcription of CHAC1 by binding directly to its promoter region

To further validate that ATF4 relies on CHAC1 to regulate HSC ferroptosis, a reverse verification was conducted by overexpressing the CHAC1 after knocking down *ATF4*. Specifically, the *CHAC1* plasmid was transfected into HSC-LX2 cells with stable knockdown of *ATF4*, followed by DHA treatment for 24 h. The *CHAC1* plasmid was subsequently used to increase CHAC1 levels. These results showed that the *CHAC1* plasmid completely counteracted the CHAC1 downregulation induced by the *ATF4* shRNA [Figure 5A]. Importantly, the downregulation of ATF4 significantly decreased the levels of markers linked to DHA-induced ferroptosis in HSCs, including iron accumulation, GSH depletion, MDA production, and lipid ROS production. Conversely, the overexpression of *CHAC1* inhibited the inhibitory effect of *ATF4* shRNA on HSC ferroptosis [Figure 5B–F]. These findings suggested that *CHAC1* served as a crucial downstream effector of ATF4 and played a significant role in regulating HSC ferroptosis.

Transcription factors bind to DNA-specific sequences (binding motifs) and activate the transcription of their target genes.[28] We further used an online tool (https://jaspar.elixir.no/) to analyze the binding sites of ATF4 and *CHAC1*. The predictions indicated the presence of two binding sites with high confidence. We cloned the *CHAC1* promoter region into a luciferase reporter system and subsequently introduced mutations. The region from −500 to +1 represents the WT *CHAC1* promoter, and the mutations are as follows: −212 to −199 bp as Mut1, −269 to −257 bp as Mut2, and the combined mutations at both positions as Mut3 [Figure 5G and H]. We determined that ATF4 could bind to the promoter region of *CHAC1* (WT) to promote its transcription. The dual-luciferase reporter system results demonstrate that the binding of ATF4 to *CHAC1* Mut1 and *CHAC1* Mut2 was significantly weakened, whereas it was nearly incapable of transactivating *CHAC1* Mut3 [Figure 5I]. These results indicated that ATF4 binds to the *CHAC1* promoter region, with primary binding sites located from −212 to −199 bp and from −269 to −257 bp.

Inhibition of CHAC1 and ATF4 attenuates DHA-induced HSC ferroptosis in vivo

To verify the role of CHAC1 and ATF4 in DHA-induced HSC ferroptosis *in vivo*, AAV8 adenovirus delivery-*Chac1* shRNA, *Atf4*-shRNA, and AAV8 adenovirus scramble (AAV8-*Chac1*-shRNA, AAV8-*Atf4*-shRNA, and AAV8-control-vector) were used to treat a mouse model of liver fibrosis induced by CCl_4. A schematic diagram of the animal treatments is shown in Supplementary Figure 4A, http://links.lww.com/CM9/C590. Photographs taken at the macroscopic level of liver tissue

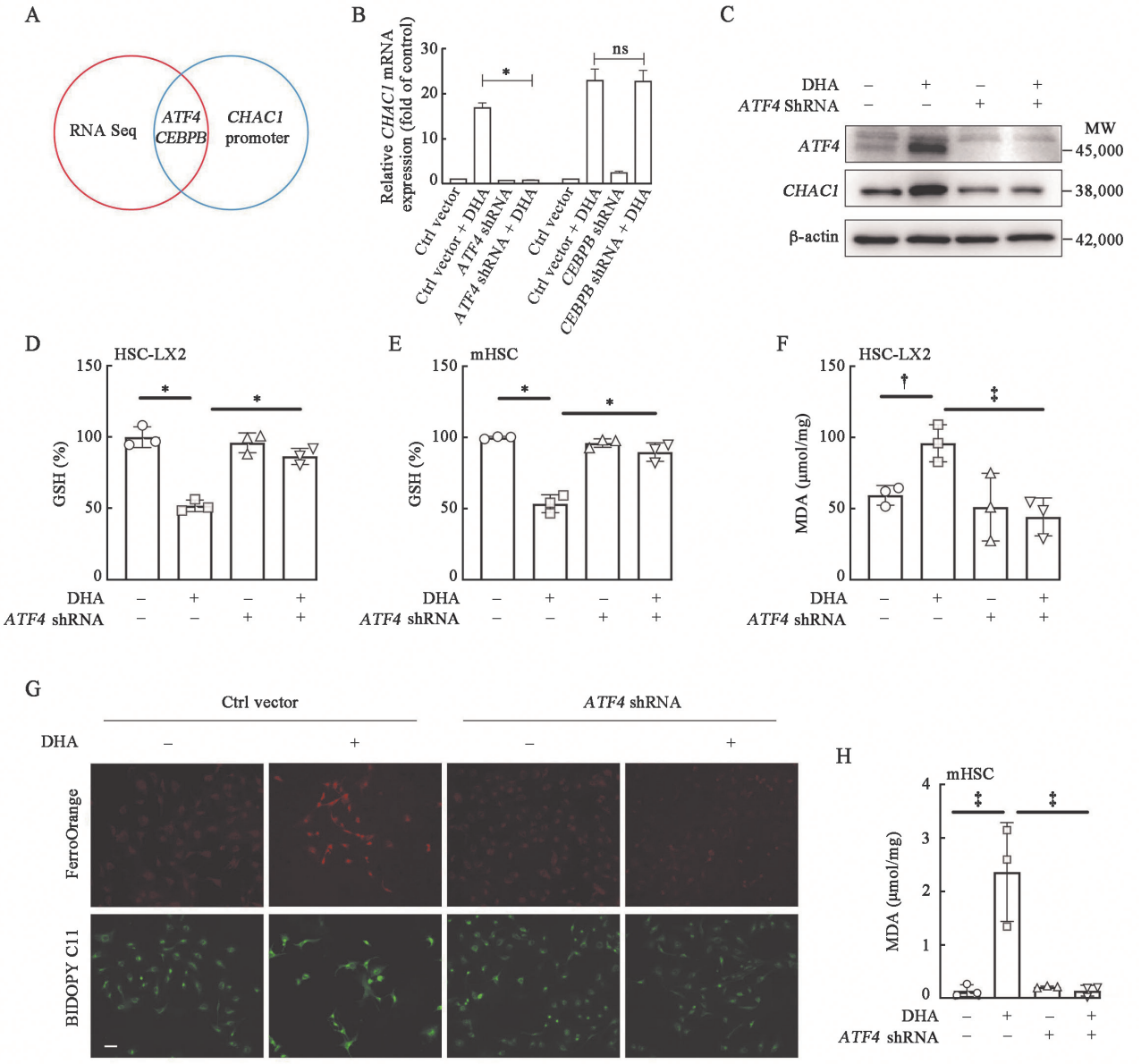

Figure 4: ATF4 is involved in regulating *CHAC1* transcription through H3K9 acetylation. (A) Venn diagram showing the overlap between the RNA-seq data and the *CHAC1* promoter. (B) The mRNA levels of *CHAC1* were measured through real-time polymerase chain reaction in HSC-LX2 cells with DHA (20 μmol/L) for 24 h. (C) The protein levels of CHAC1 were determined by Western blotting in HSC-LX2 cells with DHA (20 μmol/L) for 24 h. (D–H) GSH depletion, MDA production, iron accumulation, and lipid ROS levels were assayed in HSC-LX2 cells and mHSCs. Scale bars: 20 μm. $n = 3$ in every group. $^{*}P < 0.001$; $^{\dagger}P < 0.05$; $^{\ddagger}P < 0.01$. CHAC1: Glutathione-specific gamma-glutamylcyclotransferase 1; Ctrl: Control; CEBPB: CCAAT/enhancer binding protein beta; DHA: Dihydroartemisinin; HSC: Hepatic stellate cell; GSH: Glutathione; MDA: Malondialdehyde; mHSC: Mouse hepatic stellate cell; mRNA: messenger RNA; MW: Molecular weight; ns: Negative significant; RNA Seq: RNA sequencing; ROS: Reactive oxygen species; shRNA: Short hairpin RNA.

demonstrated that treatment with DHA significantly reduced liver fibrosis induced by CCl_4. Pretreatment with AAV8-*Chac1*-shRNA or AAV8-*Atf4*-shRNA abolished the ameliorative effect of DHA on liver fibrosis in mice [Figure 6A and Supplementary Figure 4B, http://links.lww.com/CM9/C590]. Furthermore, H&E staining, Masson's trichrome staining, and Sirius Red staining demonstrated that AAV8-*Chac1*-shRNA and AAV8-*Atf4*-shRNA significantly inhibited collagen deposition in liver fibrosis by DHA treatment [Figure 6A]. Immunohistochemical staining revealed that AAV8-*Chac1*-shRNA and AAV8-*Atf4*-shRNA significantly inhibited the effect of DHA on α-SMA expression [Figure 6B]. In addition, AAV8-*Chac1*-shRNA and AAV8-*Atf4*-shRNA diminished the inhibitory effects of DHA treatment on liver function markers, including alanine aminotransferase, aspartate aminotransferase, alkaline phosphatase, and total bilirubin [Figure 6C].

Furthermore, we extracted liver sinusoidal endothelial cells, hepatocyte macrophages, and HSCs from the livers of mice with fibrosis for further investigation. Importantly, the findings revealed that AAV8-*Chac1*-shRNA and AAV8-*Atf4*-shRNA could induce ferroptosis specifically in HSCs but not in liver sinusoidal endothelial cells, hepatocytes, or macrophages [Figure 6D and Supplementary Figure 4D, http://links.lww.com/CM9/C590]. During the course of liver fibrosis, HSCs are initially activated and

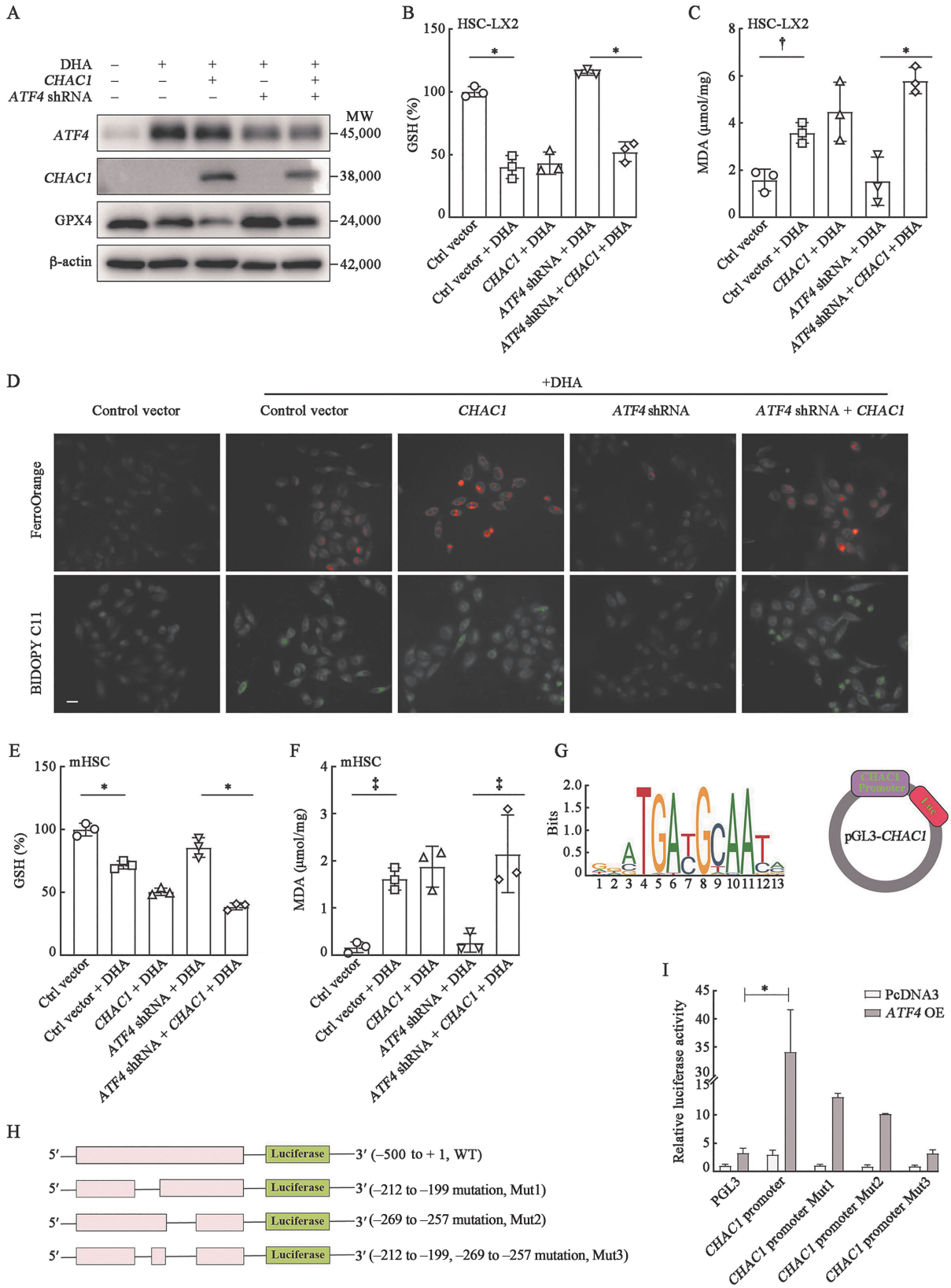

Figure 5: ATF4 promotes the transcription of *CHAC1* by binding directly to its promoter region. (A) The levels of CHAC1 and GPX4 in HSC-LX2 cells with DHA (20 μmol/L) for 24 h were determined by Western blotting. (B–F) GSH depletion, MDA production, iron accumulation, and lipid ROS levels were assayed in HSC-LX2 cells and mHSCs with DHA (20 μmol/L) for 24 h. Scale bars: 20 μm. (G) Motif analysis of the ATF4 binding peaks in the *CHAC1* promoter sequence according to the JASPAR website. The CHAC1 promoter was subsequently cloned and inserted into the PGL3 plasmid. (H) Schematic representation of the positions of the *CHAC1* promoter and mutation. (I) The luciferase activities were measured in HSC-LX2 cells with DHA (20 μmol/L) for 24 h. $n = 3$ in every group. $^{*}P < 0.001$; $^{\dagger}P < 0.05$; $^{\ddagger}P < 0.01$. CHAC1: Glutathione-specific gamma-glutamylcyclotransferase 1; DHA: Dihydroartemisinin; GPX4: Glutathione peroxidase 4; HSC: Hepatic stellate cell; GSH: Glutathione; MDA: Malondialdehyde; mHSC: Mouse hepatic stellate cell; Mut: Mutation; MW: Molecular weight; OE: Overexpression; ROS: Reactive oxygen species; shRNA: Short hairpin RNA; WT: Wild type.

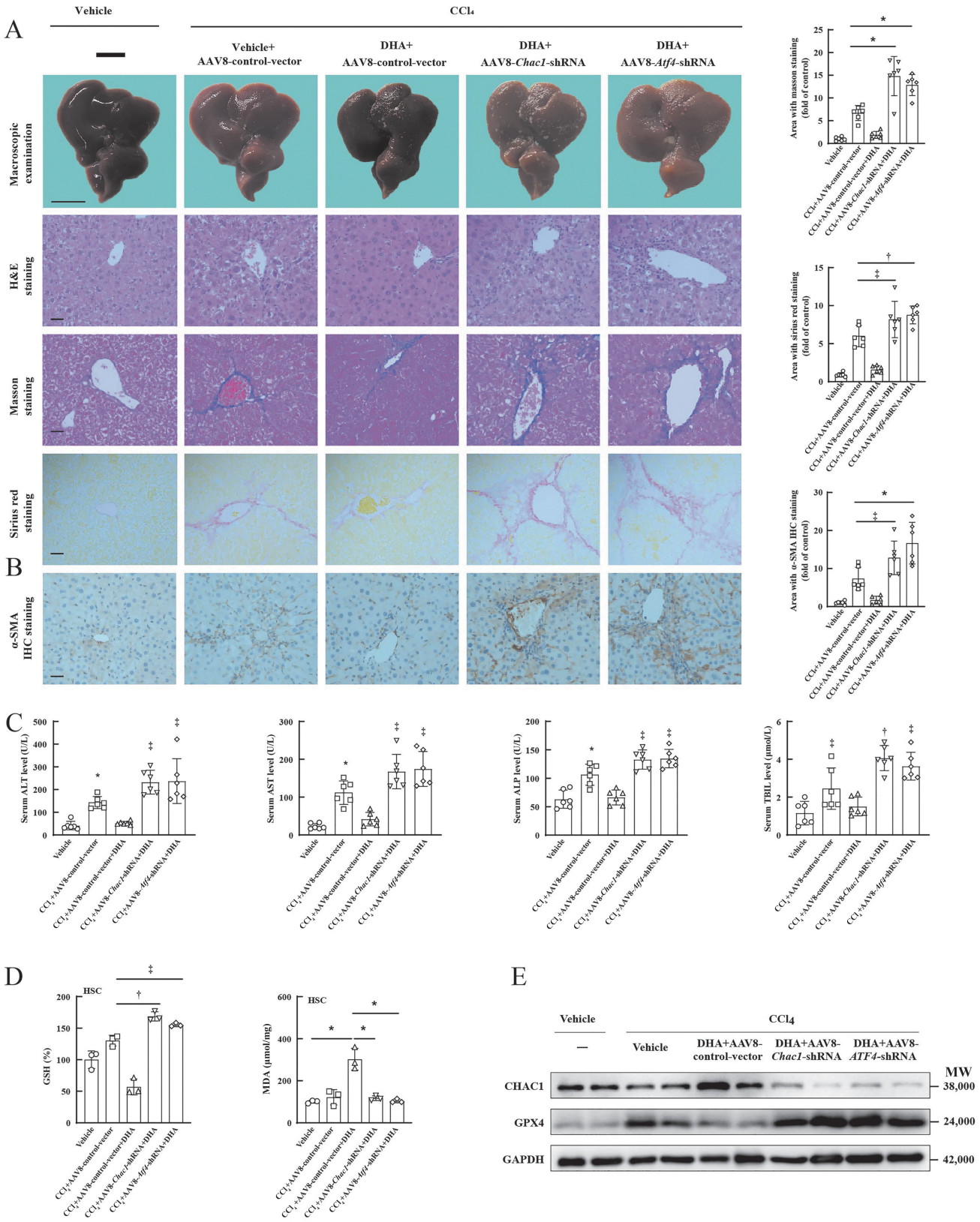

Figure 6: Inhibition of CHAC1 and ATF4 attenuated DHA-induced HSC ferroptosis *in vivo*. (A) Pathological changes in the liver were monitored visually. Scale bars: 1 cm. Histopathological examination through H&E, Masson, and Sirius Red staining. Scale bars: 50 μm. (B) α-SMA immunohistochemical staining was performed. Photographs of representative stained sections are shown. Scale bars: 50 μm. (C) Serum biochemical indices, including ALT, AST, ALP, and TBIL, were detected. (D) GSH depletion and MDA production were assayed in the mouse liver. (E) The levels of CHAC1 and GPX4 were determined by Western blotting. $n = 6$ in every group. $^{*}P < 0.001$; $^{\dagger}P < 0.01$; $^{\ddagger}P < 0.05$. ALP: Alkaline phosphatase; ALT: Alanine aminotransferase; AST: Aspartate aminotransferase; CCl_4: Carbon tetrachloride; CHAC1: Glutathione-specific gamma-glutamylcyclotransferase 1; DHA: Dihydroartemisinin; GPX4: Glutathione peroxidase 4; HSC: Hepatic stellate cell; H&E: Hematoxylin and eosin; GSH: Glutathione; MDA: Malondialdehyde; mHSC: Mouse hepatic stellate cell; MW: Molecular weight; ROS: Reactive oxygen species; shRNA: Short hairpin RNA; TBIL: Total bilirubin.

proliferate, contributing to excessive tissue scarring. Staining with Prussian blue indicated that treatment with DHA increased iron deposition in shrunken scar tissue but not in hepatocytes, whereas treatment with AAV8-*Chac1*-shRNA or AAV8-*Atf4*-shRNA abrogated the effect of DHA on iron deposition in scar tissue [Supplementary Figure 4E, http://links.lww.com/CM9/C590]. Moreover, interference with *Chac1* and *Atf4* resulted in increased GPX4 levels and diminished the inhibitory effect of DHA treatment on the expression of the fibrosis-related marker collagen I in HSCs [Figure 6E and Supplementary Figure 4C, http://links.lww.com/CM9/C590]. In conclusion, these results supported the hypothesis that CHAC1 and ATF4 regulated HSC ferroptosis in murine liver fibrosis under DHA treatment.

Discussion

Ferroptosis represents a recently identified type of regulated cell death that is driven by iron-dependent lipid peroxidation. This process fundamentally distinguishes itself from the various established forms of cell death that have been extensively studied in the past.[29] The unique characteristics of ferroptosis highlight its importance in cellular regulation and its potential implications in various pathological conditions. The increasing appreciation for the role of ferroptosis in the progression of liver fibrosis offers novel insights that could enhance both diagnostic and therapeutic strategies. Understanding how ferroptosis contributes to liver fibrosis may lead to innovative approaches for identifying at-risk patients and developing targeted treatments, thereby improving patient outcomes in patients with liver-related diseases. Interestingly, Deng *et al*[5] recently reported that the maf bZIP transcription factor G/myosin heavy chain IIa-lipocalin 2 (MafG/MYH9-LCN2) axis promotes liver fibrosis by inhibiting the ferroptosis of HSCs. Furthermore, Yang *et al*[30] reported that ATF4 promotes the activation and transdifferentiation of HSCs through endoplasmic reticulum (ER) stress-independent regulation of the epithelial mesenchymal transition (EMT) program. In agreement with earlier studies, we observed that DHA markedly reduced cell viability and mitigated liver fibrosis induced by CCl_4 through the activation of HSC ferroptosis. DHA serves as the primary extract derived from artemisinin, which is sourced from the traditional Chinese herb *Artemisia annua Linn*.[31] In addition to its established use in antimalarial treatments, DHA is currently under investigation for its potential effectiveness against various cancers, such as hepatocellular carcinoma and colorectal cancer.[32,33] Furthermore, DHA has significant antifungal and antiviral activities.[34,35] Notably, several studies have demonstrated that DHA is equipped with endoperoxide bridges that may enhance health conditions by triggering cellular ferroptosis. Ji *et al*[32] reported that DHA induces ferroptosis in hepatocellular carcinoma through the inhibition of the ATF4-solute carrier family 7 member 11 (xCT) pathway. Research has demonstrated that DHA can exert anti-hepatic fibrosis effects by inducing HSC ferroptosis. In addition to their central role in hepatic fibrosis, the functions of HSCs outside of fibrosis are equally significant. As reported by Sugimoto *et al*[36], HSCs regulate hepatocytes through R-spondin 3 and the subsequent activation of Wingless/integrated signaling, thereby controlling liver zonation, metabolism, injury, and regeneration. Investigating the novel roles of HSCs in regulating liver function may yield new insights for the treatment of liver diseases.

Various inducers can lead to ferroptosis, with the depletion of antioxidant systems being a significant contributor.[37,38] Specifically, CHAC1 plays a critical role in the management of oxidative stress through GSH, which is essential for maintaining redox balance within cells. This process is crucial, as GSH acts as a primary antioxidant that counteracts ROS. The reduction in GSH levels due to CHAC1 activity increases oxidative stress, which can result in cellular injury and apoptosis.[39,40] Furthermore, by degrading GSH, CHAC1 interferes with GPX4, an enzyme responsible for inhibiting lipid peroxidation, thereby increasing the susceptibility of cells to ferroptosis. This function holds particular importance in the cellular environment. Xue *et al*[14] reported that short-term methionine starvation accelerates ferroptosis by stimulating *CHAC1* transcription. Similarly, Wang *et al*[41] reported that ferroptosis in primary liver cancer cells is initiated by DHA, which enhances CHAC1 expression through the induction of an unfolded protein response. However, the role of CHAC1 in regulating ferroptosis in HSCs has not yet been reported. Overall, our findings provide mechanistic insights into how CHAC1 participates in HSC ferroptosis following DHA treatment.

The mechanism underlying epigenetic regulation in liver fibrosis is exceptionally intricate and encompasses a range of biological processes. These processes include DNA methylation, RNA methylation, and modifications to histones. Notably, histone acetylation stands out as the most prevalent form of epigenetic modification. This specific modification plays a crucial role in the regulation of gene transcription, influencing how various genes are expressed within the liver. Through these complex interactions, epigenetic modifications are significantly related to the progression and pathophysiology of liver fibrosis. Understanding these intricate interactions is essential for developing targeted therapies to counteract liver fibrosis. Several studies have indicated that histone acetylation is strongly correlated with human disorders and plays a significant role in the liver. For example, it has been reported that histone acetylation-mediated Na^+-taurocholate cotransporting polypeptide (NTCP) downregulation in hepatocytes is a primary event triggering liver fibrosis.[42] The levels of histone H3 acetylation decreased during ageing in the mouse liver.[43] Although the role of histone acetylation in regulating liver fibrosis has been explored, the mechanisms underlying histone acetylation in HSC ferroptosis remain poorly understood. In this study, we demonstrated that histone acetylation is increased during DHA-induced HSC ferroptosis. Notably, acetylation of histone H3 at lysine 9 is essential for the expression of *CHAC1* during DHA-induced HSC ferroptosis. Although research on how histone modifications affect ferroptosis in HSCs is limited, existing studies have demonstrated that histone modifications can regulate HSC activation through different mechanisms. It was reported that the decrease in CXXC-type zinc-finger protein 5 (CXXC5) expression

during the activation of HSCs resulted in the elimination of CpG methylation and the gain of acetylated H3K9/H3K27 on the promoter of MYC proto-oncogene like 1 (MYCL1), which in turn prompted the transactivation of MYCL1.[44] Cheng *et al*[17] reported that P300-mediated acetylation of H3K27 on the polo-like kinase 1 (PLK1) promoter is involved in HSC activation. Zheng *et al*[45] reported that the tetramerization of pyruvate kinase muscle isozyme M2 (PKM2) caused by Tetrakis-(4-ethylphenoxy)-phthalocyanine-46 (TEPP-46) successfully suppressed the activation of HSCs, diminished aerobic glycolysis, and lowered the expression levels of MYC and cyclin D1 (CCND1) by modulating the acetylation of histone H3K9 in activated HSCs. We hypothesize that different histone modifications may synergistically regulate ferroptosis. This hypothesis is based on the observation that while histone modifications may all regulate chromatin openness, the specific genes they regulate are different, thus involving distinct molecular mechanisms. Although additional experiments are needed to clarify the underlying mechanism of H3K9 acetylation in HSC ferroptosis, our study revealed the potential mechanism by which DHA regulates H3K9 acetylation in HSC ferroptosis.

Histone lysine acetylation alters the charge on histone side chains, resulting in an open chromatin configuration that allows for transcription factors to bind and enhances gene transcription.[46–48] Our study revealed that the transcription factor ATF4 was needed for the expression of CHAC1 under DHA-upregulated H3 lysine 9 acetylation. Moreover, ATF4 knockdown inhibited DHA-induced CHAC1 expression and HSC ferroptosis. Accumulating evidence has demonstrated that ATF4 is involved in ferroptosis. It was reported that ATF4 suppresses hepatocarcinogenesis by inducing solute carrier family 7 member 11 (SLC7A11) to block stress-related ferroptosis.[49] In fact, ATF4 can activate numerous genes and signaling pathways. For instance, studies have demonstrated that ATF4 induces mitochondrial stress by upregulating tribbles pseudokinase 3, leading to the activation of HSCs in rats.[50] Additionally, ATF4 has been shown to drive epithelial–mesenchymal transition gene transcription under fibrogenic conditions and that HSC-specific depletion of ATF4 suppresses liver fibrosis *in vivo*.[30] Our results contrast with those of previous reports, but this study focused on the mechanism of redox balance in HSC ferroptosis regulated by ATF4-CHAC1 under DHA-upregulated H3K9 acetylation. In addition, ATF4-regulated redox balance has been reported, and high or low expression that disrupts this balance may be harmful to the body. Wang *et al*[51] reported that ATF4 plays a critical role in the heart under conditions of hemodynamic stress by governing both cytosolic and mitochondrial production of nicotinamide adenine dinucleotide phosphate (NADPH). Although our analysis accounted for potential confounders, our study has certain limitations. We acknowledge that we did not use transgenic or gene knockout mice, which may decrease the robustness of our conclusions. Although this study demonstrated that H3K9 acetylation is crucial for DHA-regulated HSC ferroptosis in the context of liver fibrosis, the broader implications of DHA in ameliorating liver fibrosis in mice require further clarification through single-cell RNA-seq.

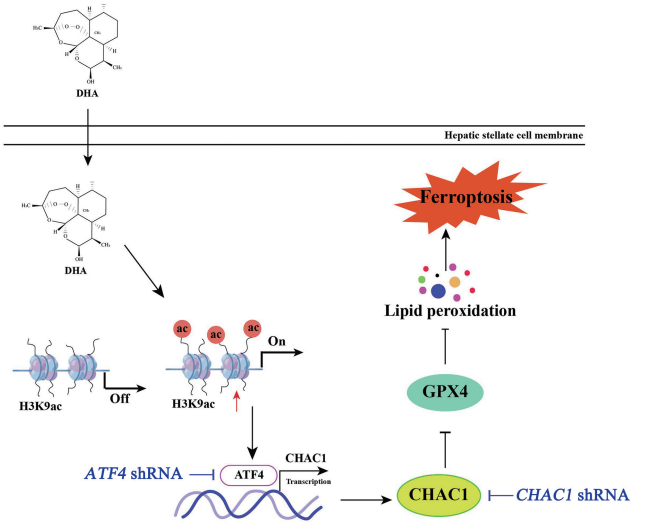

Figure 7: Upregulation of H3K9ac modification by DHA induces HSC ferroptosis by regulating *CHAC1* transcription. DHA increased H3K9ac modifications in HSCs and promoted chromatin opening. The transcription factor ATF4 promotes *CHAC1* transcription, thus triggering redox state imbalance and lipid peroxidation and eventually leading to HSC ferroptosis. ATF4: Activating transcription factor 4; CHAC1: Glutathione-specific gamma-glutamylcyclotransferase 1; DHA: Dihydroartemisinin; GPX4: Glutathione peroxidase 4; HSC: Hepatic stellate cell; shRNA: Short hairpin RNA.

In summary, we demonstrated that the histone H3K9 acetylation induced by DHA treatment results in the expression of CHAC1, which subsequently leads to lipid peroxidation and ultimately ferroptosis [Figure 7]. Previous work has demonstrated that DHA induces HSC ferroptosis through m^{6}A RNA methylation.[6] The current study reveals a fundamentally new epigenetic mechanism, DHA-triggered H3K9ac-mediated *CHAC1* transcriptional activation. These findings establish that DHA regulates HSC ferroptosis through multiple epigenetic pathways, significantly expanding the understanding of its pleiotropic effects. Although earlier studies[17–19] reported that histone modifications regulate HSC activation, our work provides novel mechanistic evidence that H3K9ac specifically governs HSC ferroptosis through the upregulation of CHAC1. Our findings may enhance the understanding of the role of histone H3K9 acetylation and ferroptosis in liver fibrosis. Furthermore, small molecules or epigenetic modulators that target CHAC1 regulation could be developed as next-generation antifibrotic drugs. DHA, an approved antimalarial drug, possesses a well-established safety profile, which may expedite its translation into clinical trials for the treatment of liver fibrosis. Given the absence of effective antifibrotic medications currently available in clinical settings, a deeper understanding of the mechanisms by which natural dietary products such as DHA function will be instrumental in the future development of therapies aimed at both preventing and treating liver fibrosis. This knowledge may pave the way for innovative approaches in drug development, leveraging the benefits of natural compounds to address this significant health challenge.

Conflicts of interest

None.

Acknowledgements

The authors thank the Animal Center of Medical College of Yangzhou University for their help.

Funding

The work was supported by grants from the National Natural Science Foundation of China (No. 82400712), the Natural Science Foundation of Jiangsu Province (No. BK20230588), the Major Project of the Natural Science Research of Jiangsu Higher Education Institutions (No. 23KJB310031), the Natural Science Foundation of Yangzhou (No. YZ2023165), the Start-up Fund from the Yangzhou University (No. 137012870), and China Postdoctoral Science Foundation (No. 2025M772730).

References

1. Yuan S, Wei C, Liu G, Zhang L, Li J, Li L, *et al*. Sorafenib attenuates liver fibrosis by triggering hepatic stellate cell ferroptosis via HIF-1α/SLC7A11 pathway. Cell Prolif 2022;55:e13158. doi: 10.1111/cpr.13158.
2. Lee EJ, Hwang I, Lee JY, Park JN, Kim KC, Kim I, *et al*. Hepatic stellate cell-specific knockout of transcriptional intermediary factor 1γ aggravates liver fibrosis. J Exp Med 2020;217:e20190402. doi: 10.1084/jem.20190402.
3. Luo P, Liu D, Zhang Q, Yang F, Wong YK, Xia F, *et al*. Celastrol induces ferroptosis in activated HSCs to ameliorate hepatic fibrosis via targeting peroxiredoxins and HO-1. Acta Pharm Sin B 2022;12:2300–2314. doi: 10.1016/j.apsb.2021.12.007.
4. Lin H, Zhou Y, Wang J, Wang H, Yao T, Chen H, *et al*. Repurposing ICG enables MR/PA imaging signal amplification and iron depletion for iron-overload disorders. Sci Adv 2021;7:eabl5862. doi: 10.1126/sciadv.abl5862.
5. Qiu X, Bi Q, Wu J, Sun Z, Wang W. Role of ferroptosis in fibrosis: From mechanism to potential therapy. Chin Med J 2024;137:806–817. doi: 10.1097/CM9.0000000000002784.
6. Shen M, Guo M, Li Y, Wang Y, Qiu Y, Shao J, *et al*. m6A methylation is required for dihydroartemisinin to alleviate liver fibrosis by inducing ferroptosis in hepatic stellate cells. Free Radic Biol Med 2022;182:246–259. doi: 10.1016/j.freeradbiomed.2022.02.028.
7. Pang Q, Zhou S, Wang Y, Pan H, Wang Z, Qin X, *et al*. GAMG alleviates liver fibrosis through inducing ferroptosis in inflammatory macrophages via the IRF1/SLC7A11 signaling pathway. Redox Biol 2025;80:103509. doi: 10.1016/j.redox.2025.103509.
8. Badgley MA, Kremer DM, Maurer HC, DelGiorno KE, Lee HJ, Purohit V, *et al*. Cysteine depletion induces pancreatic tumor ferroptosis in mice. Science 2020;368:85–89. doi: 10.1126/science.aaw9872.
9. Patel SJ, Protchenko O, Shakoury-Elizeh M, Baratz E, Jadhav S, Philpott CC. The iron chaperone and nucleic acid-binding activities of poly(rC)-binding protein 1 are separable and independently essential. Proc Natl Acad Sci U S A 2021;118:e2104666118. doi: 10.1073/pnas.2104666118.
10. Zhao X, Sun Y, Zou J, Wu Y, Huang M, Kong H, *et al*. Protein kinase A regulates ferroptosis by controlling GPX4 m(6)A modification through phosphorylation of ALKBH5. Cell Death Differ 2025;32:1058–1070. doi: 10.1038/s41418-025-01453-3.
11. Deng J, Lin X, Qin J, Li Q, Zhang Y, Zhang Q, *et al*. SPTBN2 suppresses ferroptosis in NSCLC cells by facilitating SLC7A11 membrane trafficking and localization. Redox Biol 2024;70:103039. doi: 10.1016/j.redox.2024.103039.
12. Feng L, Chen L, Wang W, Wei Q, Chen M, Jiang X, *et al*. PRMT6-mediated ADMA promotes p62 phase separation to form a negative feedback loop in ferroptosis. Theranostics 2024;14:4090–4106. doi: 10.7150/thno.94789.
13. Dong C, He Z, Liao W, Jiang Q, Song C, Song Q, *et al*. CHAC1 mediates endoplasmic reticulum stress-dependent ferroptosis in calcium oxalate kidney stone formation. Adv Sci 2025;12:e2403992. doi: 10.1002/advs.202403992.
14. Xue Y, Lu F, Chang Z, Li J, Gao Y, Zhou J, *et al*. Intermittent dietary methionine deprivation facilitates tumoral ferroptosis and synergizes with checkpoint blockade. Nat Commun 2023;14:4758. doi: 10.1038/s41467-023-40518-0.
15. Chai X, Guo J, Dong R, Yang X, Deng C, Wei C, *et al*. Quantitative acetylome analysis reveals histone modifications that may predict prognosis in hepatitis B-related hepatocellular carcinoma. Clin Transl Med 2021;11:e313. doi: 10.1002/ctm2.313.
16. Grau-Bové X, Navarrete C, Chiva C, Pribasnig T, Antó M, Torruella G, *et al*. A phylogenetic and proteomic reconstruction of eukaryotic chromatin evolution. Nat Ecol Evol 2022;6:1007–1023. doi: 10.1038/s41559-022-01771-6.
17. Cheng M, Li JJ, Niu XN, Zhu L, Liu JY, Jia PC, *et al*. BRD4 promotes hepatic stellate cells activation and hepatic fibrosis via mediating P300/H3K27ac/PLK1 axis. Biochem Pharmacol 2023;210:115497. doi: 10.1016/j.bcp.2023.115497.
18. Jain I, Brougham-Cook A, Underhill GH. Effect of distinct ECM microenvironments on the genome-wide chromatin accessibility and gene expression responses of hepatic stellate cells. Acta Biomater 2023;167:278–292. doi: 10.1016/j.actbio.2023.06.018.
19. Zhao LN, Yuan HF, Wang YF, Yun HL, Zheng W, Yuan Y, *et al*. IFN-α inhibits HBV transcription and replication by promoting HDAC3-mediated de-2-hydroxyisobutyrylation of histone H4K8 on HBV cccDNA minichromosome in liver. Acta Pharmacol Sin 2022;43:1484–1494. doi: 10.1038/s41401-021-00765-7.
20. Wang F, Chen L, Kong D, Zhang X, Xia S, Liang B, *et al*. Canonical Wnt signaling promotes HSC glycolysis and liver fibrosis through an LDH-A/HIF-1α transcriptional complex. Hepatology 2024;79:606–623. doi: 10.1097/HEP.0000000000000569.
21. Gao H, Zhou L, Zhong Y, Ding Z, Lin S, Hou X, *et al*. Kindlin-2 haploinsufficiency protects against fatty liver by targeting Foxo1 in mice. Nat Commun 2022;13:1025. doi: 10.1038/s41467-022-28692-z.
22. Luo W, Ye L, Hu XT, Wang MH, Wang MX, Jin LM, *et al*. MD2 deficiency prevents high-fat diet-induced AMPK suppression and lipid accumulation through regulating TBK1 in non-alcoholic fatty liver disease. Clin Transl Med 2022;12:e777. doi: 10.1002/ctm2.777.
23. Miao Y, Chen Y, Xue F, Liu K, Zhu B, Gao J, *et al*. Contribution of ferroptosis and GPX4's dual functions to osteoarthritis progression. EBioMedicine 2022;76:103847. doi: 10.1016/j.ebiom.2022.103847.
24. Li A, Cao C, Gan Y, Wang X, Wu T, Zhang Q, *et al*. ZNF677 suppresses renal cell carcinoma progression through N6-methyladenosine and transcriptional repression of CDKN3. Clin Transl Med 2022;12:e906. doi: 10.1002/ctm2.906.
25. Liu P, Jiang L, Kong W, Xie Q, Li P, Liu X, *et al*. PXR activation impairs hepatic glucose metabolism partly via inhibiting the HNF4α-GLUT2 pathway. Acta Pharm Sin B 2022;12:2391–2405. doi: 10.1016/j.apsb.2021.09.031.
26. Urano Y, Iwagaki A, Takeishi A, Uchiyama N, Noguchi N. Downregulation of the SREBP pathways and disruption of redox status by 25-hydroxycholesterol predispose cells to ferroptosis. Free Radic Biol Med 2025;228:319–328. doi: 10.1016/j.freeradbiomed.2025.01.010.
27. Shao Z, Bian L, Ahmadi SK, Daniel TJ, Belmonte MA, Burns JG, *et al*. Nuclear pyruvate dehydrogenase complex regulates histone acetylation and transcriptional regulation in the ethylene response. Sci Adv 2024;10:eado2825. doi: 10.1126/sciadv.ado2825.
28. Riba A, Oravecz A, Durik M, Jiménez S, Alunni V, Cerciat M, *et al*. Cell cycle gene regulation dynamics revealed by RNA velocity and deep-learning. Nat Commun 2022;13:2865. doi: 10.1038/s41467-022-30545-8.
29. Zhang C, Ding J, Lim KS, Zhou W, Miao W, Wu S, *et al*. JMJD6 rewires ATF4-dependent glutathione metabolism to confer ferroptosis resistance in SPOP-mutated prostate cancer. Cancer Res 2025;85:1496–1513. doi: 10.1158/0008-5472.can-23-2796.
30. Yang LX, Qi C, Lu S, Ye XS, Merikhian P, Zhang DY, *et al*. Alleviation of liver fibrosis by inhibiting a non-canonical ATF4-regulated enhancer program in hepatic stellate cells. Nat Commun 2025;16:524. doi: 10.1038/s41467-024-55738-1.
31. Qiu P, Chang Y, Chen X, Wang S, Nie H, Hong Y, *et al*. Dihydroartemisinin modulates enteric glial cell heterogeneity to alleviate colitis. Adv Sci 2024;11:e2403461. doi: 10.1002/advs.202403461.
32. Ji J, Cheng Z, Zhang J, Wu J, Xu X, Guo C, *et al*. Dihydroartemisinin induces ferroptosis of hepatocellular carcinoma via inhibiting ATF4-xCT pathway. J Cell Mol Med 2024;28:e18335. doi: 10.1111/jcmm.18335.

33. Dai X, Chen W, Qiao Y, Chen X, Chen Y, Zhang K, *et al*. Dihydroartemisinin inhibits the development of colorectal cancer by GSK-3β/TCF7/MMP9 pathway and synergies with capecitabine. Cancer Lett 2024;582:216596. doi: 10.1016/j.canlet.2023.216596.
34. Liang X, Chen D, Wang J, Liao B, Shen J, Ye X, *et al*. Artemisinins inhibit oral candidiasis caused by Candida albicans through the repression on its hyphal development. Int J Oral Sci 2023;15:40. doi: 10.1038/s41368-023-00245-0.
35. Marchesi E, Gentili V, Bortolotti D, Preti L, Marchetti P, Cristofori V, *et al*. Dihydroartemisinin-ursodeoxycholic bile acid hybrids in the fight against SARS-CoV-2. ACS Omega 2023;8:45078–45087. doi: 10.1021/acsomega.3c07034.
36. Sugimoto A, Saito Y, Wang G, Sun Q, Yin C, Lee KH, *et al*. Hepatic stellate cells control liver zonation, size and functions via R-spondin3. Nature 2025;640:752–761. doi: 10.1038/s41586-025-08677-w.
37. Gao M, Monian P, Pan Q, Zhang W, Xiang J, Jiang X. Ferroptosis is an autophagic cell death process. Cell Res 2016;26:1021–1032. doi: 10.1038/cr.2016.95.
38. Li N, Yi X, He Y, Huo B, Chen Y, Zhang Z, *et al*. Targeting ferroptosis as a novel approach to alleviate aortic dissection. Int J Biol Sci 2022;18:4118–4134. doi: 10.7150/ijbs.72528.
39. Perra L, Balloy V, Foussignière T, Moissenet D, Petat H, Mungrue IN, *et al*. CHAC1 is differentially expressed in normal and cystic fibrosis bronchial epithelial cells and regulates the inflammatory response induced by pseudomonas aeruginosa. Front Immunol 2018;9:2823. doi: 10.3389/fimmu.2018.02823.
40. Sun Y, Atmadibrata B, Yu D, Wong M, Liu B, Ho N, *et al*. Upregulation of LYAR induces neuroblastoma cell proliferation and survival. Cell Death Differ 2017;24:1645–1654. doi: 10.1038/cdd.2017.98.
41. Wang Z, Li M, Liu Y, Qiao Z, Bai T, Yang L, *et al*. Dihydroartemisinin triggers ferroptosis in primary liver cancer cells by promoting and unfolded protein response-induced upregulation of CHAC1 expression. Oncol Rep 2021;46:240. doi: 10.3892/or.2021.8191.
42. Garrido A, Kim E, Teijeiro A, Sánchez P, Gallo R, Nair A, *et al*. Histone acetylation of bile acid transporter genes plays a critical role in cirrhosis. J Hepatol 2022;76:850–861. doi: 10.1016/j.jhep.2021.12.019.
43. Oliviero G, Kovalchuk S, Rogowska-Wrzesinska A, Schwämmle V, Jensen ON. Distinct and diverse chromatin proteomes of ageing mouse organs reveal protein signatures that correlate with physiological functions. ELife 2022;11:e73524. doi: 10.7554/eLife.73524.
44. Wu X, Dong W, Kong M, Ren H, Wang J, Shang L, *et al*. Down-regulation of CXXC5 de-represses MYCL1 to promote hepatic stellate cell activation. Front Cell Dev Biol 2021;9:680344. doi: 10.3389/fcell.2021.680344.
45. Zheng D, Jiang Y, Qu C, Yuan H, Hu K, He L, *et al*. Pyruvate kinase M2 tetramerization protects against hepatic stellate cell activation and liver fibrosis. Am J Pathol 2020;190:2267–2281. doi: 10.1016/j.ajpath.2020.08.002.
46. Wei G, Abraham BJ, Yagi R, Jothi R, Cui K, Sharma S, *et al*. Genome-wide analyses of transcription factor GATA3-mediated gene regulation in distinct T cell types. Immunity 2011;35:299–311. doi: 10.1016/j.immuni.2011.08.007.
47. Han T, Zhuo M, Yuan C, Xiao X, Cui J, Qin G, *et al*. Coordinated silencing of the Sp1-mediated long noncoding RNA MEG3 by EZH2 and HDAC3 as a prognostic factor in pancreatic ductal adenocarcinoma. Cancer Biol Med 2020;17:953–969. doi: 10.20892/j.issn.2095-3941.2019.0427.
48. Tsou PS, Palisoc PJ, Ali M, Khanna D, Sawalha AH. Genome-wide reduction in chromatin accessibility and unique transcription factor footprints in endothelial cells and fibroblasts in scleroderma skin. Arthritis Rheumatol 2021;73:1501–1513. doi: 10.1002/art.41694.
49. He F, Zhang P, Liu J, Wang R, Kaufman RJ, Yaden BC, *et al*. ATF4 suppresses hepatocarcinogenesis by inducing SLC7A11 (xCT) to block stress-related ferroptosis. J Hepatol 2023;79:362–377. doi: 10.1016/j.jhep.2023.03.016.
50. Ye MP, Lu WL, Rao QF, Li MJ, Hong HQ, Yang XY, *et al*. Mitochondrial stress induces hepatic stellate cell activation in response to the ATF4/TRIB3 pathway stimulation. J Gastroenterol 2023;58:668–681. doi: 10.1007/s00535-023-01996-7.
51. Wang X, Zhang G, Dasgupta S, Niewold EL, Li C, Li Q, *et al*. ATF4 protects the heart from failure by antagonizing oxidative stress. Circ Res 2022;131:91–105. doi: 10.1161/CIRCRESAHA.122.321050.

How to cite this article: Shen M, Han WS, Cai LL, Gong WJ, Qian L. H3K9 acetylation-dependent *CHAC1* transcription in dihydroartemisinin-induced hepatic stellate cell ferroptosis. Chin Med J 2026;139:93–107. doi: 10.1097/CM9.0000000000003788